Optics Letters

Hollow-core fiber with stable propagation delay between −150 °C and +60 °C

Zitong Feng,* Hesham Sakr, John R. Hayes, Eric Numkam Fokoua, Meng Ding, Francesco Poletti, David J. Richardson, and Radan Slavík

Optoelectronics Research Centre, University of Southampton, Southampton, SO17 1BJ, UK
**Corresponding author: Zitong.Feng@soton.ac.uk*

Received 13 October 2022; revised 1 December 2022; accepted 14 December 2022; posted 15 December 2022; published 27 January 2023

Optical fibers with a low thermal coefficient of delay (TCD) have been developed for frequency and timing transmission/distribution. However, their temperature sensitivity changes as a function of temperature and, to date, no study of such fibers has demonstrated improved performance over extended temperature ranges, especially at sub-zero temperatures. Here, we show that a hollow core fiber (HCF) with a thin acrylate coating can have a TCD within ±2.0 ps/km/°C over a broad temperature range from −150°C to +60°C. In addition, this thinly coated HCF can be fully insensitive to temperature around −134°C, making it of interest, e.g., for laser stabilization close to cryogenic temperatures.

https://doi.org/10.1364/OL.478183

Optical fiber based timing synchronization and frequency distribution have improved measurement accuracy in various fields such as fundamental physics, navigation, astronomy, and geodesy [1–3]. The main challenge in transmitting a stable timing/frequency signal through an optical fiber is the signal phase and delay variation due to changes in the fiber's optical path length caused by acoustic, mechanical, and thermal perturbations. For continuous wave or narrow-bandwidth signals, the optical path length is usually stabilized using passive or active compensation of carrier optical frequency [4,5]. For synchronization using short pulses such as in large-scale scientific infrastructures, e.g., x ray free-electron lasers (XFEL) [6], extreme light infrastructure (ELI) [7], and multi-telescope array projects [8], optical/electrical delay lines [9,10] are used for propagation time stabilization. The delay lines required for such stabilization need a relatively high dynamic range to compensate for the large thermal sensitivity of standard single-mode fibers (SMFs) which typically have a thermal coefficient of delay (TCD) of approximately 40 ps/km/°C. For example, the European XFEL has 24 fiber link channels with 24 sets of compensation units, each incorporating a 31-cm-long free space delay line [11]. The delay line dynamic range needs to be even larger for longer links, for example, synchronization of distant telescopes, e.g., Ref. [12], where a tunable delay line consisting of a 10-km-long thermally controlled fiber spool was used to compensate a 110-km installed SMF link. Such compensation was reported to induce additional noise and thus degradation of the transmission line stability [12].

Optical fibers with reduced TCD compared to SMF can reduce the accumulated delay variation and their use thus enables compensating delay lines with smaller dynamic range. There are several such fibers available commercially. They are marketed as "phase stable optical fibers" and their performance is typically given in terms of TCD. The term "phase" here refers to the phase of an optical pulse envelope (i.e., propagation time) rather than the optical phase directly. For consistency with our previous publications, however, we use the term "phase sensitivity" when referring to optical phase (related to effective refractive index) and delay (related to the group refractive index). All of the commercially available low-TCD fibers achieve TCD reduction by using specialty coatings. Unfortunately, these coatings have strongly temperature-dependent properties and generally can be optimized only over relatively narrow temperature ranges. Such fibers are commercially available from Furukawa (TCD = 2.5–5.0 ps/km/°C), Linden Photonics (5.1–6.5 ps/km/°C [13]), and Yangtze Optical FC (2.3–9.2 ps/km/°C [14]). The TCD of these fibers has only been reported over limited temperature ranges in the literature, e.g., 5–40°C (Furukawa and Linden) and −20–40°C for Yangtze Optical FC. Even over these limited temperature ranges, their thermal sensitivity changes significantly with temperature, which may, for example, lead to reduced Square Kilometer Array (SKA) system performance operating in the desert, where the air temperature may change between −12 and 43°C in a single day [15]. Other challenging environments include regions with extremely low temperatures, for example far-North/South, high altitude (e.g., for telescopes), or even polar regions. Applications there include long offset glacier sounding by synchronizing bistatic radar [16] and military radar array in polar regions (e.g., North warning system) [17] which require passive sub-ns level time synchronization.

An alternative approach is to use hollow core optical fibers (HCFs) that have attenuation comparable or even lower than SMF [18,19], in which the TCD is inherently low, around 2 ps/km/°C at room temperature. This is thanks to the removal of the glass material form the air core which virtually removes

the contribution from the thermo-optic effect, the biggest contributor to the thermal sensitivity of standard fibers [20]. The TCD of uncoated HCF was demonstrated to be further reduced at lower temperatures and even reached zero around −71°C [21]. However, the TCD of an HCF with a standard acrylate coating was actually shown to increase at low temperatures, an effect attributed to a large increase in coating stiffness at low temperatures, which significantly increases the coating's contribution to the overall fiber TCD. The coating is typically in a soft rubbery state at room temperature but undergoes a phase transition into a glassy state at low temperatures. A TCD of 15 ps/km/°C was reported over the temperature range of −70 to −80°C for an HCF with standard coating [21].

In this Letter, we demonstrate an HCF with a thin (10 μm) acrylate coating and measure a TCD within ±2 ps/km/°C over the temperature range from −150 to +60°C. To the best of our knowledge, this is the lowest reported fiber TCD over such a broad range of temperatures. In addition, we show that its phase thermal sensitivity S_φ crosses zero at −134°C, confirming the predictions made in [21]. This will be of interest in applications where zero-crossing thermal sensitivity at low temperatures is desired, for example, in interferometry. At low temperatures, the thermal noise is reduced, which may be of interest, e.g., for stabilization of ultra-stable lasers [22,23].

The thinly coated HCF sample was 40 m long and was manufactured in-house, with a nested antiresonant nodeless fiber (NANF) geometry for which our team has reported attenuation levels as low as 0.22 dB/km [19]. The fabricated HCF had a silica glass diameter of 185 μm [24].

The TCD characterizes how optical signal propagation time τ through a fiber of unity length changes with temperature. To measure this with just the tens of meters of fiber length that we had available would require highly accurate propagation time measurement [25]. Alternatively, it can be quantified by measuring the light's phase thermal sensitivity S_φ in an interferometer as we show below.

According to [26], length-normalized phase sensitivity is

$$S_\varphi = \frac{2\pi}{\lambda}\left(\frac{dn_{eff}}{dT} + \frac{n_{eff}}{L}\frac{dL}{dT}\right), \tag{1}$$

where λ is the wavelength, n_{eff} is the effective refractive index, and L is the fiber length. The first term on the right-hand side of Eq. (1) is due to the thermo-optic effect that can be neglected in a sealed (with closed ends) HCF [25]. The group v_g and phase v_p velocities are related as follows [27]:

$$v_g = v_p + k\frac{dv_p}{dk}, \tag{2}$$

where $k = 2\pi/\lambda$ is the angular wavenumber. The light propagation time τ and its accumulated phase φ can be expressed as

$$\tau = \mathrm{L}/v_g, \quad \varphi = k \cdot n_{eff} \cdot L. \tag{3}$$

Subsequently, the TCD and S_φ are related as follows:

$$TCD = \frac{1}{L}\frac{d\tau}{dT} = \frac{1}{L}\frac{d\left(\frac{L}{v_g}\right)}{dT} = -\frac{\lambda^2}{2\pi c}\frac{d\left(\frac{d\varphi}{dT}\right)}{d\lambda} = -\frac{\lambda^2}{2\pi c}\frac{d(S_\varphi)}{d\lambda}. \tag{4}$$

Substituting Eq. (1) into Eq. (4) and neglecting the contribution from the thermo-optic effect as discussed above, we obtain

$$TCD = \frac{\lambda}{2\pi c}\cdot S_\varphi - \frac{\lambda}{cL}\cdot\frac{dL}{dT}\cdot\frac{dn_{eff}}{d\lambda}. \tag{5}$$

The n_{eff} as a function of wavelength calculated using a finite element mode solver (COMSOL) [28] for a NANF-type fiber is shown in Fig. 1. From this data, we obtain $\frac{dn_{eff}}{d\lambda} = 7\times10^{-7}$/nm in the wavelength range from 1500 to 1600 nm. Considering this value and $\frac{dL}{dT} = 0.3$ ppm/°C [24], we found that the second term in Eq. (5) is three orders of magnitude smaller than the first one in our NANF and thus can be neglected, giving

$$TCD \approx \frac{\lambda}{2\pi c}\cdot S_\varphi. \tag{6}$$

Under the above considerations (sealed HCF of NANF type), the TCD can be directly obtained from the phase thermal sensitivity S_φ.

Our experimental setup is shown in Fig. 2. An imbalanced Mach–Zehnder interferometer (MZI) was built with the thinly coated HCF in the delay arm. To ensure that any changes in the differential phase between the two MZI arms are attributed to the thinly coated HCF only, we carefully balanced the pigtail lengths of the fiber couplers and locked the interrogating narrow linewidth laser (1555 nm, Rock laser from NP Photonics) to a carrier-envelope-stabilized optical frequency comb (Menlo FC1500-250). The HCF sample was placed inside a 14-cm diameter glass Petri dish. The Petri dish was fixed to the top of a dual-walled polystyrene box, which was then filled with liquid nitrogen (LN_2) to just below the bottom of the Petri dish. After closing the two polystyrene boxes, the LN_2 cools the interferometer down to −190°C. However, as it evaporates and its level lowers, the temperature of the interferometer slowly increases. After all the LN_2 has evaporated the temperature

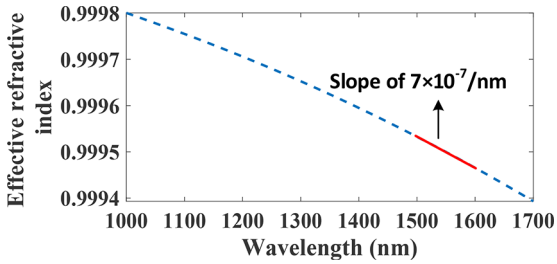

Fig. 1. Calculated effective refractive index n_{eff} of the fundamental mode of the NANF-type HCF used in our experiments as a function of wavelength.

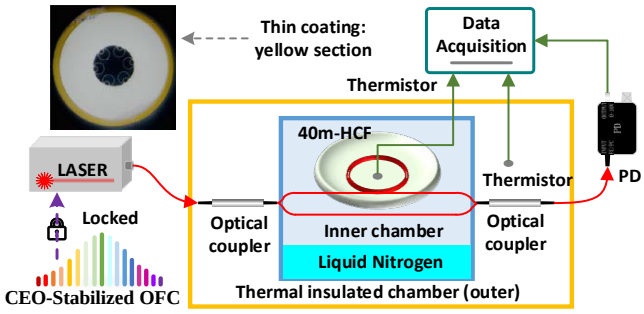

Fig. 2. Experimental setup. Light from a laser frequency locked to an optical frequency comb (OFC) passes through a Mach–Zehnder interferometer that incorporates 40-m HCF in the delay arm. CEO, carrier-envelope offset; PD, photodiode; HCF, hollow-core fiber.

steadily increases until it reaches the ambient level. By simultaneously monitoring the temperature and the intensity at the output of the MZI, the phase thermal sensitivity can then be calculated as [21]

$$S_\varphi = \frac{1}{L}\frac{d\varphi}{dT} = \frac{number\,of\,fringes \cdot 2\pi}{\Delta T \cdot L}, \tag{7}$$

where the ΔT is the temperature change over the observation time and L is the length of the thinly coated HCF. Let us consider that the minimum change we can resolve is when the interference fringe moves by one half (e.g., from a minimum to a maximum). This corresponds to propagation time change of 2.5 fs (at 1555 nm), which is approximately 400 times more accurate than typically achievable in the time-of-flight measurement of the TCD [25] with 1-ps resolution.

The TCD calculated using Eq. (6) from the measured S_φ [Eq. (7)] is shown in Fig. 3, where for comparison, the published TCD of Furukawa, Linden Photonics, and Yangtze Optical FC low-TCD fibers are also shown. The detailed temperature ranges and their TCD are also summarized in Table 1. We see in Fig. 3 that the thinly coated HCF has a low TCD within ±2.0 ps/km/°C (S_φ within ±2.4 rad/m/°C) over a very broad temperature range from −150°C to +60°C. For higher temperatures, e.g., up to 115°C, the TCD is also <2 ps/km/°C, even when the HCF has a thicker coating, e.g., 75 μm as reported in [29] and shown in Fig. 3. This is in contrast to the three commercially available low-TCD fibers, for which the TCD is larger and changes

Table 1. Low-TCD Fibers from Furukawa, Linden Photonics, and YOFC, SMF (250-μm Coated Diameter), and 10-μm Coated HCF (Thinly Coated HCF) Presented Here

Fiber type	TCD (ps/km/°C), 5–40°C	TCD (ps/km/°C), −20–40°C
SMF	38–46	38–49
Furukawa	2.5–5.0	Not available
Linden Photonics	5.1–6.5	Not available
Yangtze Optical FC	3.8–9.2	2.3–9.2
HCF, 10 μm (This work)	1.6–1.7	1.5–1.7

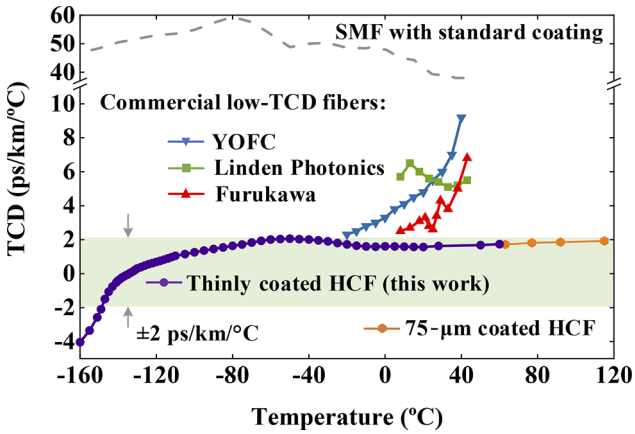

Fig. 3. Measured TCD of a thinly coated HCF. For comparison, we also show reported data for low-TCD fibers from Furukawa, Linden Photonics, and Yangtze Optical FC ([13], [14]), an SMF with standard acrylate coating (coated fiber diameter of 250 μm) [21], and an HCF with 75-μm coating at temperatures above 60°C [29].

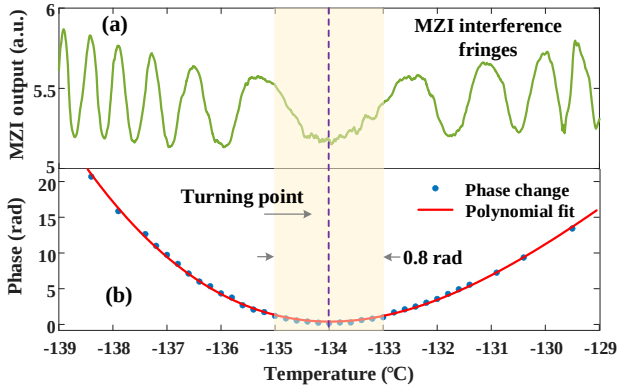

Fig. 4. (a) Measured MZI interference fringes in the vicinity of the thermal sensitivity zero crossing and (b) calculated phase change (blue scatters) with the third-order polynomial fit (red line).

significantly within a relatively narrow temperature range of 0–40°C. Considering the temperature range from 5°C to 40°C (over which data are available for all these fibers), the TCD changes by 2.5, 1.4, and 5.4 ps/km/°C for fibers from Furukawa, Linden Photonics, and Yangtze Optical FC, respectively. This is an over ten times larger change relative to the thinly coated HCF for which the TCD changes by only 0.1 ps/km/°C over the same temperature range.

In addition to low TCD, the thinly coated HCF shows another interesting property, which has been already predicted for such a fiber in Ref. [21]. Both its S_φ and TCD (already shown in Fig. 3) cross the zero sensitivity point at low temperatures. This is of interest in stable interferometry, where keeping fibers at such zero-temperature sensitivity can enable the realization of temperature-insensitive fiber interferometers. This zero crossing is shown in Fig. 4(a), where we show the measured output power of the MZI at temperatures close to the TCD zero crossing of −134°C. The spacing between the fringes changes significantly as the temperature changes, from narrow to very wide near −134°C, then becoming narrow again. The extracted phase [using Eq. (5)] is shown in Fig. 4(b). The accumulated phase first decreased, reaching a turning point at approximately −134°C, corresponding to zero thermal sensitivity, then increased. The accumulated phase change within ±1°C around −134°C is only 0.8 rad, indicating stable (less than π phase variation) phase. The data are well fit by a third-order polynomial [also shown in Fig. 4(b)], from which we extracted a phase slope of 1×10^{-8}°C^{-2}.

Figure 5 shows the phase thermal sensitivity S_φ over the −180°C to +20°C temperature range for the measured thinly coated HCF and compares it to values published for 50-μm coated HCF and bare HCF [21]. The expected sensitivity obtained by interpolating the bare and 50-μm coated HCF results [21] are also shown. The measured thinly coated HCF S_φ agrees with the expected value from room temperature down to approximately −150°C, including the zero sensitivity predicted to occur at −135°C and achieved experimentally at −134°C.

In conclusion, we have demonstrated for the first time, a thinly coated HCF with a low TCD over an unprecedentedly broad temperature range. We measured values within ±2.0 ps/km/°C for the temperature range from −150°C (i.e., below the lowest outdoor temperature ever recorded on Earth, which is −91.2°C) to +60°C. The influence of such a thin coating on the fiber mechanical strength is yet to be assessed rigorously. However,

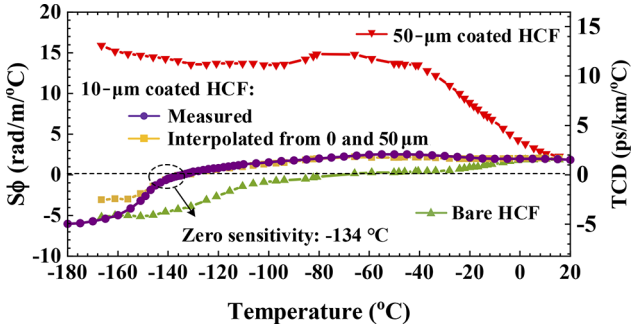

Fig. 5. Measured phase thermal sensitivity S_φ of thinly coated HCF with the corresponding TCD shown on the right y axis. For comparison, previously reported measured data for bare HCF, HCF with 50-μm, and S_φ extrapolated from 0 and 50-μm data for a 10-μm coated HCF [21] are also shown.

in our experiment, it was significantly more robust than uncoated fibers, without any breakages during several months when coiled to 14-cm diameter, including a dozen −190–20°C temperature cycles. It is worth mentioning that we also coiled this thinly coated fiber on a glass cylinder under tension [30] without experiencing any breakages. Additionally, fibers with similar coating thickness (albeit using different material such as polyimide, e.g., SM1550P from Thorlabs, or metal, e.g., CU1300 from IFG fiber) are available commercially and offer good mechanical stability. The measured low values of TCD over such a broad temperature range can greatly reduce the compensating delay line dynamic range, or provide a passive synchronization solution for phase array radar applications. It can also greatly extend the performance of systems requiring a low-TCD fiber, in environments reaching low temperatures or experiencing a large temperature change over a short time. Such places include, for example, polar regions, permafrost regions, or deserts. We expect that for practical use, a cable with a loose buffer construction could be designed to mechanically protect the fiber while not degrading its thermal stability.

In addition, we demonstrated experimentally that thinly coated HCF can achieve zero phase thermal sensitivity S_φ at −134°C. Based on interpolation of available data, the zero sensitivity temperature could be shifted by controlling the coating thickness, e.g., to the N_2 boiling point. Additionally, the slope of the thermal phase sensitivity S_φ around −134°C is 1×10^{-8}°C^{-2}, which is slightly lower than what has been measured in other low-sensitivity systems operating at low temperatures, e.g., crystalline silicon cavities operating at −149°C, 1.7×10^{-8}°C^{-2} [22] and an SMF interferometer operating at −270°C, 2.2×10^{-8} °C^{-2} [23]. This further enhances the attractiveness of fiber for future precision experiments.

Funding. European Research Council (682724); Engineering and Physical Sciences Research Council (EP/P030181/1).

Disclosures. The authors declare no conflicts of interest.

Data availability. The data for this work will be accessible through the University of Southampton Institutional Research Repository [31].

REFERENCES

1. B. M. Roberts, P. Delva, A. Al-Masoudi, A. Amy-Klein, C. Baerentsen, C. Baynham, E. Benkler, S. Bilicki, S. Bize, and W. Bowden, New J. Phys. **22**, 093010 (2020).
2. Ł. Śliwczyński, P. Krehlik, and M. Lipiński, Meas. Sci. Technol. **21**, 075302 (2010).
3. K. Predehl, G. Grosche, S. Raupach, S. Droste, O. Terra, J. Alnis, T. Legero, T. Hänsch, T. Udem, and R. Holzwarth, Science **336**, 441 (2012).
4. L. Hu, X. Tian, G. Wu, and J. Chen, Opt. Lett. **45**, 4308 (2020).
5. X. Wang, Z. Liu, S. Wang, D. Sun, Y. Dong, and W. Hu, Opt. Lett. **40**, 2618 (2015).
6. M. Y. Peng, P. T. Callahan, A. H. Nejadmalayeri, S. Valente, M. Xin, L. Grüner-Nielsen, E. M. Monberg, M. Yan, J. M. Fini, and F. X. Kärtner, Opt. Express **21**, 19982 (2013).
7. G. Mourou and T. Tajima, Science **331**, 41 (2011).
8. D. Dravins, T. Lagadec, and P. D. Nuñez, Nat. Commun. **6**, 6852 (2015).
9. P. Krehlik, Ł. Śliwczyński, Ł. Buczek, and J. Kołodziej, IEEE Trans. Ultrason., Ferroelect., Freq. Contr. **66**, 163 (2019).
10. O. Lopez, A. Amy-Klein, M. Lours, C. Chardonnet, and G. Santarelli, Appl. Phys. B **98**, 723 (2010).
11. T. Lamb, M. Czwalinna, M. Felber, C. Gerth, T. Kozak, J. Müller, H. Schlarb, S. Schulz, C. Sydlo, and M. Titberidze, Proc. IPAC **19**, 3835 (2019).
12. N. Cheng, W. Chen, Q. Liu, D. Xu, F. Yang, Y.-Z. Gui, and H.-W. Cai, Chin. Phys. B **25**, 014206 (2016).
13. M. Bousonville, M. Bock, M. Felber, T. Ladwig, T. Lamb, H. Schlarb, S. Schulz, C. Sydlo, S. Hunziker, and P. Kownacki, in *Proc. Beam Instrum. Workshop* (JACoW, 2012), pp. 109–111.
14. "Phase Stable Optical Cable"https://en.yofc.com/view/2356.html
15. X. Zhu, B. Wang, Y. Guo, Y. Yuan, R. Gamatham, B. Wallace, K. Grainge, and L. Wang, Chin. Opt. Lett. **16**, 010605 (2018).
16. N. L. Bienert, D. M. Schroeder, S. T. Peters, E. J. MacKie, E. J. Dawson, M. R. Siegfried, R. Sanda, and P. Christoffersen, IEEE Trans. Geosci. Remote Sensing **60**, 1 (2022).
17. "North Warning System," Wikipedia, 2023, https://en.wikipedia.org/wiki/North_Warning_System
18. G. T. Jasion, H. Sakr, J. R. Hayes, S. R. Sandoghchi, L. Hooper, E. N. Fokoua, A. Saljoghei, H. C. Mulvad, M. Alonso, A. Taranta, T. D. Bradley, I. A. Davidson, Y. Chen, D. J. Richardson, and F. Poletti, in *Optical Fiber Communication Conference 2022* (IEEE, 2022), 1–3.
19. H. Sakr, T. D. Bradley, G. T. Jasion, E. N. Fokoua, S. R. Sandoghchi, I. A. Davidson, A. Taranta, G. Guerra, W. Shere, and Y. Chen, in *Optical Fiber Communication Conference* (Optica Publishing Group, 2021), F3A. 4.
20. R. Slavík, G. Marra, E. N. Fokoua, N. Baddela, N. V. Wheeler, M. Petrovich, F. Poletti, and D. J. Richardson, Sci. Rep. **5**, 15447 (2015).
21. W. Zhu, E. R. N. Fokoua, A. A. Taranta, Y. Chen, T. Bradley, M. N. Petrovich, F. Poletti, M. Zhao, D. J. Richardson, and R. Slavík, J. Lightwave Technol. **38**, 2477 (2020).
22. T. Kessler, C. Hagemann, C. Grebing, T. Legero, U. Sterr, F. Riehle, M. Martin, L. Chen, and J. Ye, Nat. Photonics **6**, 687 (2012).
23. B. Merkel, D. Repp, and A. Reiserer, Opt. Lett. **46**, 444 (2021).
24. B. Shi, H. Sakr, J. Hayes, X. Wei, E. N. Fokoua, M. Ding, Z. Feng, G. Marra, F. Poletti, and D. J. Richardson, Opt. Lett. **46**, 5177 (2021).
25. E. N. Fokoua, W. Zhu, M. Ding, Z. Feng, Y. Chen, T. D. Bradley, G. T. Jasion, D. J. Richardson, F. Poletti, and R. Slavík, J. Lightwave Technol. **39**, 2142 (2021).
26. E. N. Fokoua, M. N. Petrovich, T. Bradley, F. Poletti, D. J. Richardson, and R. Slavík, Optica **4**, 659 (2017).
27. U. Gliese, S. Norskov, and T. Nielsen, IEEE Trans. Microwave Theory Tech. **44**, 1716 (1996).
28. H. Sakr, Y. Chen, G. T. Jasion, T. D. Bradley, J. R. Hayes, H. C. H. Mulvad, I. A. Davidson, E. Numkam Fokoua, and F. Poletti, Nat. Commun. **11**, 6030 (2020).
29. R. Slavík, E. N. Fokoua, M. Bukshtab, Y. Chen, T. Bradley, S. R. Sandoghchi, M. Petrovich, F. Poletti, and D. Richardson, Opt. Lett. **44**, 4367 (2019).
30. M. Ding, E. N. Fokoua, J. R. Hayes, H. Sakr, P. Horak, F. Poletti, D. J. Richardson, and R. Slavík, Opt. Lett. **47**, 2510 (2022).
31. Z. Feng, H. Sakr, J. R. Hayes, E. N. Fokoua, M. Ding, F. Poletti, D. J. Richardson, and R. Slavík, "Hollow-core fiber with stable propagation delay between −150℃ and +60℃: Data," University of Southampton Institutional Research Repository , (2023), https://doi.org/10.5258/SOTON/D2511.